

P..812

On the Knotting Probability of Random Equilateral Hexagons

Ani Nadiga, Clara Buck, and Sean Gallagher

May 20 2019

1 Introduction to Topological Knots

What is a knot? Let us step inside the vast universe of \mathbb{R}^3 . Before we embark on this adventure, let us reflect on where we are coming from. We see knots all over our world. When you tie your shoes, that is a knot. When your headphones are tangled, that is a knot. When Ani ties a knot, that is a knot. But are these actually knots or not? The land of topology says no. Imagine a world where your string is attached together at the ends. Now untying your shoes will prove much more difficult; perhaps even impossible. This motivates the following definition.

Definition 1. A *topological knot* is an embedding of a circle in \mathbb{R}^3 .

In topology, we consider the "string" to be infinitely thin and infinitely stretchable. Two knots are *equivalent* if one can be deformed to the other by stretching and twisting without creating any self-intersections or breaking the string.

Definition 2. A knot is an *unknot* if it is equivalent to the planar circle. A *non-trivial knot* is any knot that is not the unknot.

. We will often represent knots with two dimensional representations called knot diagrams. See figure 1.

Definition 3. A *knot diagram* is a regular projection of a knot in which crossing information is given by small gaps.

Knots are often classified based on their *crossing number*, which is the smallest number of crossings a diagram of a knot can have. The crossing number is an example of a knot invariant.

Definition 4. A *knot invariant* is some function associated with a given knot that doesn't change under any deformations.

It is possible that different knots may have the same value for a certain knot invariant. For example, there are multiple distinct knots with 5 crossings. We have several other characteristics to help us describe knots:

Definition 5. If we choose a direction to follow through the knot then the knot has an *orientation*.

Definition 6. A knot is *invertible* if it can be deformed to have reverse orientation.

Definition 7. A knot is *achiral* or *amphicheiral* if it can be deformed to its mirror image. We say a knot is *chiral* if it is not achiral.

Note that deforming a knot to its mirror image is the same as switching all the crossings from over to under and vice versa.

Definition 8. A knot is *reversible* if it is invertible and chiral

We would like to represent the possible deformations of a knot in \mathbb{R}^3 using just manipulations of the knot projection. Reidemeister moves allow give us explicit rules for how we can manipulate a projection. There are three Reidemeister moves. Any legal deformation of a knot in \mathbb{R}^3 can be represented a sequence of Reidemeister moves in the knot diagram.

1.1 Trefoils

The simplest type of non trivial-knot is a trefoil, since it is the only type of knot with only three crossings and there are no knots with only one or two crossings.

Theorem 1. Topological trefoils are reversible (invertible and chiral).

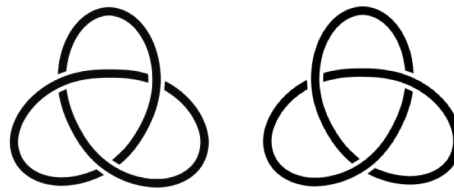


Figure 1: A left-handed trefoil (left) and a right-handed trefoil (right).

In other words, if we give a trefoil an orientation, we can deform it to have reverse orientation. However, we cannot deform it to its mirror image. Thus there are actually two distinct types of trefoils, which we refer to as left-handed and right-handed.

2 Introduction to Geometric Knots

2.1 Geometric Knots and Stick Numbers

There are many applications of knot theory. For example, there is evidence that molecules of DNA sometimes form non-trivial knots, as shown in figure 2.

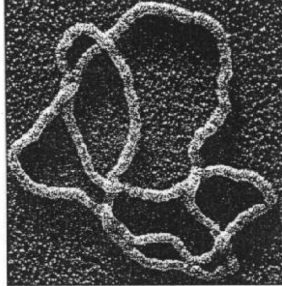


Figure 2: A molecule of DNA forming a trefoil knot.

Unlike most structures found in nature, topological knots are infinitely thin and infinitely stretchable. In order to understand certain applications of knot theory, we may want a model with greater rigidity. This is one motivation for the following definition.

Definition 9. *A geometric knot is a polygon in \mathbb{R}^3 , consisting of n straight edges and no self-intersections.*

Geometric knots are similar to topological knots, but with straight edges. They are sometimes referred to as *stick knots*, since they resemble a collection of sticks stuck together end to end. For the remainder of this paper, when we say *knot* we will be referring to geometric knots.

Definition 10. *A geometric knot is a **geometric unknot** if it can be deformed to a regular planar polygon without breaking, bending, or intersecting any of the edges.*

Definition 11. *The **minimal stick number** of a topological knot is the smallest number of edges required to realize the knot.*

For example, to form a trefoil you need at least 6 edges, so the minimal stick number of a trefoil is 6. The minimal stick number of the figure-eight knot is 7. See figure 3.

Theorem 2. *You need at least 6 edges to construct a non-trivial geometric knot, and the only non-trivial knot with 6 edges is the trefoil.*

We ought to be careful when creating and reading knot diagrams. Figure 4 seems to show a non-trivial knot made using only 5 sticks. However, if we carefully follow the edges we will notice that every edge rises up as it crosses over another, but at no point do we come back down. Hence the picture is just an optical illusion, and doesn't represent an actually pentagon.

2.2 The space of Geometric Knots

Every geometric knot is a polygon in \mathbb{R}^3 . We can represent any n -sided polygon in \mathbb{R}^3 as a point in \mathbb{R}^{3n} by first choosing a distinguished vertex v_1 , called the

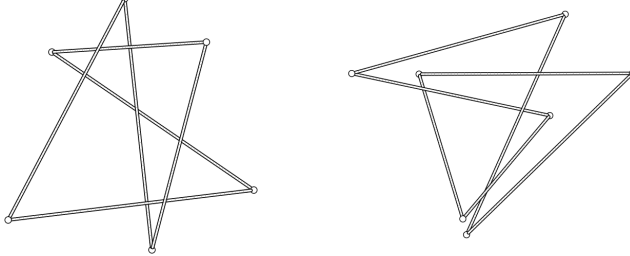


Figure 3: A 6-sided trefoil (left) and a 7-sided figure-eight knot (right).

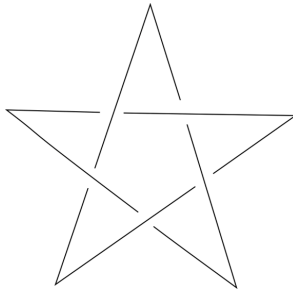


Figure 4: A deceptive 5 stick knot.

root, and an orientation, and then listing the coordinates of the vertices starting at the root and going in the direction of the orientation. We label the vertices v_1, v_2, \dots, v_n and the edges $\overline{12}, \overline{23}, \dots, \overline{n1}$. Not every point in \mathbb{R}^{3n} represents a knot because some of the points correspond to polygons with a pair of intersecting edges. This motivates the following two definitions:

Definition 12. $\mathbf{Geo}^{(n)}$ is the space of all geometric knots.

Definition 13. The **discriminant** of \mathbb{R}^{3n} , Σ^n , is the set of all polygons with at least one pair of intersecting edges.

This gives us the subspace

$$\mathbf{Geo}^{(n)} = \mathbb{R}^{3n} - \sum^n \quad (1)$$

a $3n$ -dimensional manifold. We call two polygons geometrically equivalent if one can be continuously deformed into the other while remaining an n -sided polygon the entire time. We can formalize this using paths in $\mathbf{Geo}^{(n)}$.

Definition 14. A **path** in $\mathbf{Geo}^{(n)}$ is a continuous map from the interval $[0, 1]$ to $\mathbf{Geo}^{(n)}$.

To understand this definition, first note that if there is some point that is very close to another in $\mathbf{Geo}^{(n)}$, the first is a slightly deformed version of the second. Thus, a continuous mapping h from $[0,1]$ to $\mathbf{Geo}^{(n)}$ represents continuously changing the polygon $h(0)$ until it reaches $h(1)$.

Definition 15. *If there is a path between two points of $\mathbf{Geo}^{(n)}$, then we say that the polygons that they represent are geometrically equivalent.*

Geometric equivalence, like topological equivalence, is an equivalence relation. This means that $\mathbf{Geo}^{(n)}$ can be partitioned into disjoint components, where any two elements of the same component are path connected. If two polygons are geometrically equivalent then they lie in the same component of $\mathbf{Geo}^{(n)}$.

Now we will take a more formal look at the discriminant (the space of polygons that contain self intersection). A polygon (v_a, v_b, \dots, v_n) is in \sum^n if some arbitrary edge $\overline{12}$ intersects another arbitrary edge $\overline{34}$, in which case it will satisfy,

$$\begin{aligned}(v_2 - v_1) \times (v_3 - v_1) \cdot (v_4 - v_1) &= 0 \\ (v_2 - v_1) \times (v_3 - v_1) \cdot (v_2 - v_1)(v_4 - v_1) &< 0 \\ (v_4 - v_3) \times (v_1 - v_3) \cdot (v_4 - v_3)(v_2 - v_3) &< 0.\end{aligned}$$

2.3 Equilateral Knots

Paths in $\mathbf{Geo}^{(n)}$ do not preserve edge length, that is, lengths may be stretched or shrunk indefinitely. We may want to impose greater rigidity by fixing the edge length. Specifically, we consider the space $\mathbf{Eql}^{(n)}$.

Definition 16. $\mathbf{Eql}^{(n)}$ is the space of all hexagonal knots with all edges of length 1.

We can construct $\mathbf{Eql}^{(n)}$ from $\mathbf{Geo}^{(n)}$ by considering the function $f : \mathbf{Geo}^{(6)} \rightarrow \mathbb{R}^n$ where

$$f(v_1, \dots, v_n) = (||v_2 - v_1||, \dots, ||v_n - v_1||). \quad (2)$$

For $(v_1, \dots, v_n) \in \mathbf{Geo}^{(n)}$, f gives a vector containing the side lengths of each edge of the polygon. Thus we can define:

$$\mathbf{Eql}^{(6)} = f^{-1}(1, 1, \dots, 1). \quad (3)$$

Recall that $\mathbf{Geo}^{(n)}$ is $3n$ -dimensional. With the addition of edge-length condition, we lose n dimensions.

Theorem 3. $\mathbf{Eql}^{(n)}$ is a $2n$ -dimensional submanifold of $\mathbf{Geo}^{(n)}$

We can formalize paths in $\mathbf{Eql}^{(n)}$ in the same way as in $\mathbf{Geo}^{(n)}$.

Definition 17. A **path** in $\mathbf{Eql}^{(n)}$ is a continuous map from the interval $[0, 1]$ to $\mathbf{Eql}^{(n)}$.

A path in $\mathbf{Eqr}^{(n)}$ is different from one in $\mathbf{Geo}^{(n)}$. In $\mathbf{Geo}^{(n)}$, we can stretch the edge lengths as we move through a path, but in $\mathbf{Eqr}^{(n)}$ the edges are fixed throughout the path. As with $\mathbf{Geo}^{(n)}$, two knots are *equilaterally equivalent* if there is a path in $\mathbf{Eqr}^{(n)}$ between them.

For $3 \leq n \leq 5$, both $\mathbf{Geo}^{(n)}$ and $\mathbf{Eqr}^{(n)}$ have exactly one component, that of unknots, as expected given *Theorem 2*. In other words, given any geometric knot with $3 \leq n \leq 5$ sides, it can be deformed to a planar polygon through a path in $\mathbf{Geo}^{(n)}$. If it is equilateral, it can be deformed to a planar regular polygon through a path in $\mathbf{Eqr}^{(n)}$.

2.4 Path-Components of $\mathbf{Geo}^{(6)}$ and $\mathbf{Eqr}^{(6)}$

Recall that there are two topological components of trefoils: right-handed and left-handed trefoils. Since trefoils can be constructed using only 6 edges, we must have at least three components in $\mathbf{Geo}^{(6)}$ (unknots, left-handed trefoils, and right-handed trefoils).

Theorem 4 (Calvo 2001). *$\mathbf{Geo}^{(6)}$ has 5 path-components. One component consists of unknots, two components consist of right-handed trefoils and two components consist of left-handed trefoils.*

These additional components are the first evidence that geometric knottedness is different from topological knottedness. There are two different types of right-handed hexagonal trefoils, while there is only one component of right-handed topological trefoils.

The two components of right handed hexagonal trefoils is a result of our choice of root (v_1). In other words, if one takes a physical configuration of a hexagon and chooses a root and an orientation, and then shifts the root by one, the resulting hexagon will be in a different component of $\mathbf{Geo}^{(6)}$ from the original hexagon. By *Theorem 2.5 (Calvo, 2001)*, if we consider some subgroup Γ of the dihedral group $\prec r, s \succ$, then $\mathbf{Geo}^{(6)}/\Gamma$ has only three components if and only if Γ is not contained in $\prec s^2, rs \succ$. That is, if we allow for some combination of rotation and reflection that is not in the stabilizer, then we dissolve the boundary between the two extra components.

We can now classify $\mathbf{Eqr}^{(6)}$ in a similar way. Recall that two hexagons are equilaterally equivalent if there is a path between them in $\mathbf{Eqr}^{(6)}$.

Theorem 5 (Calvo, 2001). *Two equilateral hexagons are equilaterally equivalent if and only if they are geometrically equivalent.*

Thus there are at least as many path components of $\mathbf{Eqr}^{(6)}$ as there are of $\mathbf{Geo}^{(6)}$. In fact, $\mathbf{Eqr}^{(6)}$ has the same number of components as $\mathbf{Geo}^{(6)}$.

Theorem 6 (Calvo, 2001). *$\mathbf{Eqr}^{(6)}$ has 5 path components.*

By combining these two theorems, we know that each of the five components of $\mathbf{Geo}^{(6)}$ contains a single connected component of $\mathbf{Eqr}^{(6)}$, as depicted in Figure 5.

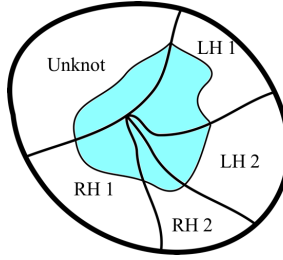


Figure 5: The five components of $\mathfrak{Geo}^{(n)}$ with the submanifold $\mathfrak{Egu}^{(n)}$ shaded.

2.5 The Knot Invariant

We want to distinguish between the five path components of $\mathfrak{Egu}^{(6)}$. In order to describe the combinatorial knot invariant we must discuss two new concepts: *chirality* and *curl*. The knot invariant, sometimes referred to as *joint chirality-curl*, will allow us to distinguish between the different components of $\mathfrak{Geo}^{(6)}$, and thus also between the components of $\mathfrak{Egu}^{(6)}$.

2.5.1 Chirality

Chirality will allow us to distinguish between unknots, left-handed trefoils and right-handed trefoils. Consider a hexagon $H = \langle v_1, v_2, v_3, v_4, v_5, v_6 \rangle$. Let T_2 refer to the triangular disc determined by the vertices v_1, v_2 , and v_3 , and oriented by the “right hand rule” wrapping from lower to higher numbered vertices. We define T_4 and T_6 in the same way as the triangles with v_4 and v_6 respectively as the middle vertices. We will describe everything in terms of T_2 for now, but one can easily generalize the idea for T_4 and T_6 .

We define Δ_2 , the algebraic intersection number of T_2 , as the sum of all piercings of T_2 , where a positive piercing (in accordance with the right hand rule) has value $+1$ and a negative piercing has value -1 . Notice that T_2 can only be pierced by edges that don’t share a vertex with the triangular disc itself. Thus only edges $\overline{45}$ and $\overline{56}$ can pierce T_2 . But because both of those edges are adjacent, they cannot pierce in the same direction without requiring one of them to bend. So it follows that Δ_2 must take on values of either $-1, 0$, or $+1$.

Definition 18. *The chirality of a hexagon is the product of the three algebraic piercing numbers, $\Delta_2\Delta_4\Delta_6$.*

This can take on values of $-1, 0$, or $+1$, but it actually turns out that if the chirality is $+1$ then all three algebraic intersection numbers are $+1$, and vice versa for -1 chirality. Thus we have the following result showing how these three values fully identify the topological knot type of H .

Theorem 7 (Calvo, 2001). *Let H be a hexagon. Then*

- (I) *H is a right-handed trefoil $\iff \Delta_2 = \Delta_4 = \Delta_6 = 1$.*
- (II) *H is a left-handed trefoil $\iff \Delta_2 = \Delta_4 = \Delta_6 = -1$.*
- (III) *H is an unknot $\iff \Delta_i = 0$ for some $i \in \{2, 4, 6\}$.*

2.5.2 Curl

The **curl** distinguishes within the two components of right handed trefoils and within the two components of left handed trefoils. Recall that unlike topological trefoils, rooted oriented hexagonal trefoils are not reversible, which is a result of picking a root vertex. This is what gives us the two extra components in $\mathfrak{Geo}^{(6)}$, that **curl** will allow us to identify.

Definition 19. *The curl of a hexagon is the sign of the z-coordinate of v_2 when v_1 , v_3 , and v_5 are placed counterclockwise in the xy-plane. Thus*

$$\text{curl}H = \text{sign}((v_3 - v_1) \times (v_5 - v_1) \cdot (v_2 - v_1)).$$

The sign of the z-coordinate of v_2 tells us whether a trefoil is positive curl or negative curl. By *Corollary 2.3 (Calvo, 2001)*, this classification is invariant under geometric deformations. Even though it is based only on v_2 , it actually tells us about the location of v_4 and v_6 too.

Lemma 8. *If H is a trefoil and v_1 , v_3 , and v_5 are oriented counterclockwise in the xy-plane, then the sign of the z-coordinate of v_2 will be the same as that of v_4 and v_6*

Proof. We must show that if H is a positive curl trefoil, then all three evenly numbered vertices will be above the xy -plane. A nearly identical argument will exist for negative curl.

Suppose H is a positive curl trefoil. Then by definition v_2 lies above the plane. Lets assume that H is a trefoil with chirality +1, with confidence that a similar argument can be made for -1. Thus T_2 is pierced by the edge $\overline{45}$. But v_5 lies in the plane, so since the entire interior of the disc T_2 is above the plane, it follows that v_4 lies above the plane.

Then the interior of T_4 must be above the plane, and $\overline{61}$ must pierce T_4 . Since v_6 is in the plane, it follows that v_6 must be above the plane. \square

2.5.3 The Knot Invariant

We combine chirality and curl into what is sometimes called the *joint chirality-curl*, which is our combinatorial knot invariant.

Definition 20. *The joint chirality-curl of a hexagon H is the ordered pair $\mathcal{J}(H) = (\Delta_2\Delta_4\Delta_6, \Delta_2^2\Delta_4^2\Delta_6^2\text{curl}(H))$*

Note that the multiplier in front of $\text{curl}(H)$ just ensures that the term is 0 if H is an unknot. The values of this ordered pair will correctly classify the component of $\mathfrak{Geo}^{(6)}$ that a given hexagonal knot falls under.

Theorem 9 (Calvo, 2001). *The joint chirality-curl is an invariant of hexagons under geometric deformations. The geometric knot type of a hexagon H is completely determined by the value of its joint chirality-curl, since $\mathcal{J}(H) = (0, 0)$ iff H is an unknot; $\mathcal{J}(H) = (+1, c)$ iff H is a right-handed trefoil with $\text{curl}H = c$; and $\mathcal{J}(H) = (-1, c)$ iff H is a left-handed trefoil with $\text{curl}H = c$.*

This follows from the fact that both curl and chirality are invariant under geometric deformations. Note that while this knot invariant by definition distinguishes between the five components of $\text{Geo}^{(6)}$, it also distinguishes between the five components of $\text{Egu}^{(6)}$ since two hexagons that are geometrically equivalent in $\text{Geo}^{(6)}$ are also equivalent in $\text{Egu}^{(6)}$.

We can derive more information about the four components of trefoils. We are able to identify which edges must be piercing each triangular disk T_2 , T_4 , and T_6 . This will be helpful in efficiently allowing us to classify a random hexagon. We identify the piercings, shown in the following tables, through a similar analysis as in the proof of *Lemma 8*.

$$\mathcal{J}(H) = (+1, +1):$$

Triangle	Pieced By
T_2	$\overline{45}$
T_4	$\overline{61}$
T_6	$\overline{23}$

$$\mathcal{J}(H) = (+1, -1):$$

Triangle	Pieced By
T_2	$\overline{56}$
T_4	$\overline{12}$
T_6	$\overline{34}$

$$\mathcal{J}(H) = (-1, +1):$$

Triangle	Pieced By
T_2	$\overline{56}$
T_4	$\overline{12}$
T_6	$\overline{34}$

$$\mathcal{J}(H) = (-1, -1):$$

Triangle	Pieced By
T_2	$\overline{45}$
T_4	$\overline{61}$
T_6	$\overline{23}$

3 Some Symplectic Geometry

A manifold is a topological space that is locally homeomorphic to \mathbb{R}^n . A symplectic manifold is an even dimensional manifold with a closed non-degenerate two form, typically denoted ω . If there is a Hamiltonian circle action on a manifold M , then there exists a moment map $\mu : M \rightarrow \mathbb{R}$. For any $x \in M$, $\mu(x)$ is a quantity associated with x that is invariant over the orbit of x . In general, if you have a product of k such circle actions there is a map $\mu : M \rightarrow \mathbb{R}^k$. Now $\mu(x)$ is a k -dimensional vector associated with x that is invariant over the orbit of x . When k is half of the dimension of M , we call M a toric-symplectic manifold.

The image of μ will always form a convex moment polytope, \mathcal{P} . The vertices of \mathcal{P} correspond to points in M that are invariant under the torus action. If we can invert μ we get the action-angle map $\alpha : \mathcal{P} \times T^n \rightarrow M$.

For example if M is the unit 2-sphere with ω the standard area form, then M is a symplectic manifold. Then if we define the circle action to be a rotation of the sphere about the z -axis we get a toric symplectic manifold. In this case, the moment map, $\mu : S^2 \rightarrow \mathbb{R}$, returns the z -coordinate of any point, and the moment polytope is the interval $[-1, 1]$. The endpoints of this polytope, -1 and 1 , correspond the fixed points of the circle action, the north and south pole. The inverse of the moment map is $\alpha : [-1, 1] \times S^1 \rightarrow S^2$.

The following theorem will be helpful in a number of instances.

Theorem 10 (Duistermaat–Heckman). *Suppose M is a $2n$ -dimensional toric symplectic manifold with moment polytope \mathcal{P} , T^n is the n -torus (n copies of the circle) and α inverts the moment map. If we take the standard measure on the n -torus and the uniform (or Lebesgue) measure on $\text{int}(\mathcal{P})$, then the map $\alpha : \text{int}(\mathcal{P})T^n M$ parametrizing a full measure subset of M in action-angle coordinates is measure-preserving. In particular, if $f : M\mathbb{R}$ is any integrable function then*

$$\int_M f(x)dm = \int_{\mathcal{P} \times T^n} f(d_1, \dots, d_n, \theta_1, \dots, \theta_n) d\text{Vol}_{\mathbb{R}^n} d\theta_1 \wedge \dots \wedge d\theta_n$$

. If $f(d_1, \dots, d_n, \theta_1, \dots, \theta_n) = f_d(1, \dots, d_n) f_\theta(\theta_1, \dots, \theta_n)$, then

$$\int_M f(x)dm = \int_{\mathcal{P}} f_d(d_1, \dots, d_n) d\text{Vol}_{\mathbb{R}^n} \int_{T^n} f_\theta(\theta_1, \dots, \theta_n) d\theta_1 \wedge \dots \wedge d\theta_n$$

4 Action Angle Coordinates

We can describe any equilateral hexagon by listing its 6 vertices: $v_1, v_2, v_3, v_4, v_5, v_6$. This representation has two draw backs. First, it is inefficient. It requires 18 numbers (three for each vertex), but the space of equilateral hexagons up to translation and rotation is 6-dimensional. Requiring that the edge lengths are fixed gives us 6 additional equations which reduces the space to 12 dimensions. Modding out by translations removes 3 dimensions and modding out by rotations removes another 3 dimensions, which leaves us with 6 dimensions.

Listing the vertices also makes it difficult to randomly generate hexagons. It is not obvious how to pick 6 points such that they form a hexagon with unit edge lengths. *Cantarella* and *Shonkwiler* (2016) gives a 6-dimensional parameterization of the space of equilateral hexagons. We will first give some intuition behind their method before going more formally into the details.

We first must pick a triangulation of the hexagon. There are five triangulations to choose from. In order to best harmonize with the knot invariant, we will use the triangulation shown in Figure 6.

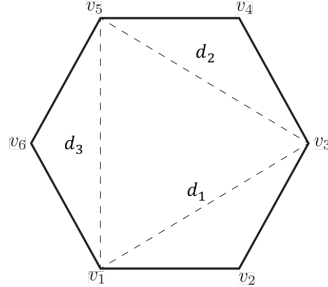


Figure 6: The chosen triangulation of the regular planar hexagon

Then we can stretch or shrink the diagonal lines that compose the triangulation, and "fold" the other triangles through some angle around each of those lines. While not immediately obvious, it will turn out that any hexagon, up to translation and rotation, can be realized in this manner. Thus, we can describe any hexagonal knot as a point with 6 coordinates: three that describe the lengths of the diagonal lines (d_1, d_2, d_3) and three for the angles ($\theta_1, \theta_2, \theta_3$).

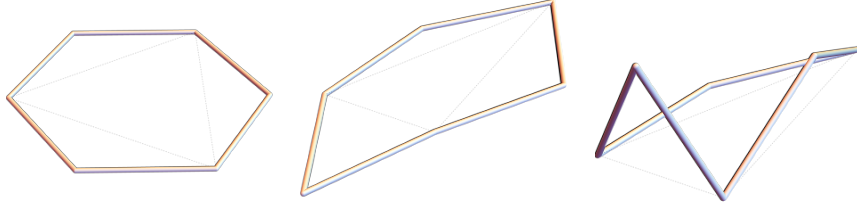


Figure 7: Triangulating the hexagon (left), stretching and shrinking along the dotted line (middle), and folding the triangles (right)

4.1 Action-Angle Coordinates

These 6 coordinates that describe an equilateral hexagon are called the action-angle coordinates. A generic point is denoted $(d_1, d_2, d_3, \theta_1, \theta_2, \theta_3)$. Each point corresponds to a unique equilateral hexagon up to translation and rotation. To construct the hexagon, create a triangle with side lengths d_1, d_2 , and d_3 . We call this triangle \mathcal{T} . Next we make the three triangles T_2, T_4, T_6 (the subscript denotes which vertex of the hexagon is uniquely contained in the given triangle). These triangles each have one side of length d_1, d_2 , and d_3 , respectively, and two sides of length 1. Next we "glue" each of these triangles to \mathcal{T} , as shown below. We want to do this in such a way that the resulting hexagon is planar. There are two ways to do this. Intuitively, one is where all of T_2, T_4 , and T_6 are placed on the "outside" of \mathcal{T} , and the other is the configuration where the triangles are folded inward. We choose for them to be folded inward. More formally, we glue the triangles in such a way that the interiors of each of T_2, T_4 , and T_6 intersect the interior of \mathcal{T} .

Now we will rotate each of T_2, T_4 , and T_6 about the line that joins them to \mathcal{T} through angles θ_1, θ_2 , and θ_3 , respectively. In order to do this we must define an orientation for the rotations. We say that the initial configuration is when all of the angles are 0. Then as the angles increase from 0, the triangles T_2, T_4 , T_6 will come above the plane containing \mathcal{T} .

Note that this construction gives an injective function from the space of action-angle coordinates to the space of equilateral hexagons in \mathbb{R}^3 up to translation and rotation. Thus, to complete our parametrization of equilateral hexagons in \mathbb{R}^3 , we must show that every such hexagon can be constructed using some action-angle coordinate.

Theorem 11. *Every rooted and oriented equilateral hexagon in \mathbb{R}^3 can be described using action angle coordinates, up to translation and rotation.*

Proof. Consider any rooted oriented hexagon v_1, v_2, \dots, v_6 in \mathbb{R}^3 . Then we can recover the action-angle coordinates that correspond to that hexagon in the following way. Let P be the plane containing v_1, v_3 and v_5 . Then let d_1, d_2 , and d_3 be the lengths of the segments $\overline{13}$, $\overline{35}$, and $\overline{51}$, respectively. Let \mathbf{n} be the vector $\overline{13} \times \overline{14}$, $\mathbf{n}_2 = \overline{12} \times \overline{13}$, $\mathbf{n}_4 = \overline{34} \times \overline{35}$, and $\mathbf{n}_6 = \overline{56} \times \overline{51}$. Then let θ_1, θ_2 , and θ_3 be the angles between \mathbf{n} and \mathbf{n}_2 , \mathbf{n} and \mathbf{n}_4 , and \mathbf{n} and \mathbf{n}_6 , respectively. Thus the action-angle coordinates $(d_1, d_2, d_3, \theta_1, \theta_2, \theta_3)$ uniquely describe the given hexagon. \square

4.2 Visualizing the Space of Action-Angle Coordinates

Each point in the space of action-angle coordinates has 6 coordinates. The first three describe lengths and the last three describe angles. So we will visualize this space as the union of two three dimensional spaces, one for the lengths, and one for the angles.

4.2.1 The Moment Polytope, \mathcal{P}

Not all choices of d_1, d_2 , and d_3 correspond to realizable equilateral hexagons. The four triangles in Figure 6 must cooperatively satisfy 6 triangle inequalities. Since the side lengths of the hexagon are all 1, we must have $0 \leq d_i \leq 2$ for each d_i . The inner triangle \mathcal{T} must satisfy three triangle inequalities: $d_1 \leq d_2 + d_3$, $d_2 \leq d_1 + d_3$, and $d_3 \leq d_1 + d_2$.

These 6 inequalities give a bounded region in \mathbb{R}^3 , called the *moment polytope*, \mathcal{P} . Every tuple (d_1, d_2, d_3) corresponding to a valid choice of diagonal lengths is contained in \mathcal{P} . The moment polytope has volume 4, which is exactly half of the volume of the cube containing it.

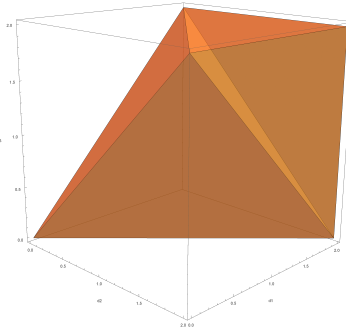


Figure 8: The moment polytope for the chosen triangulation, contained inside of the cube of side length 2

Note that points on the boundary of \mathcal{P} correspond to singularities, so when sampling we are concerned only with the interior. For example, if $d_i = 2$ for any i , then the angle between two edges of the hexagon must be π , making a length 2 straight segment, so the hexagon would actually be a pentagon. Furthermore, given certain $(\theta_1, \theta_2, \theta_3)$, there will be points (d_1, d_2, d_3) in the interior of the moment polytope corresponding to non-embedded polygons (polygons with at least one pair of intersecting edges). However, the space of these points has measure 0.

4.2.2 The Three Torus, T^3

We need to sample tuples $(\theta_1, \theta_2, \theta_3)$ where $0 < \theta_i < 2\pi$. The three-torus T^3 describes this space. T^3 is a product of 3 circles, $S^1 \times S^1 \times S^1$. Choosing one point from each circle gives us three angles. We can represent T^3 as a cube, as in 9, where we identify opposite faces.

In this construction there appears to be a difference between 2π and 0. For example, the point $(0, 0, 2\pi)$ appears to be different from $(0, 2\pi, 0)$. Since $0 = 2\pi$, these points are actually the same. This is why the opposite sides of the cube are identified to form a three dimensional torus. To actually connect up these pairs of faces visually would require a fourth dimension. We can sample the last three coordinates of any point in the space of action-angle coordinates by sampling a point in the the three dimensional torus represented as a cube.

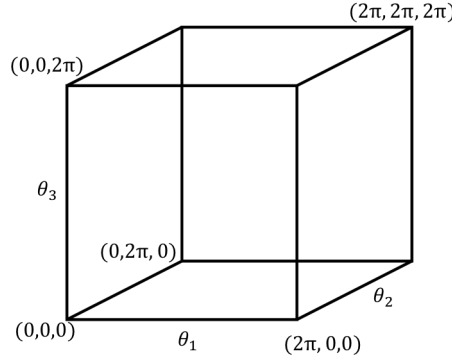


Figure 9: The 3-Torus T^3 represented by a cube with identified faces. T^3 contains all tuples $(\theta_1, \theta_2, \theta_3)$ with $0 < \theta_i < 2\pi$.

4.3 The Symplectic Geometry of $\mathfrak{E}\mathfrak{qu}(n)$

Let $\text{Pol}(6)$ denote the space of all equilateral possibly singular hexagons up to translation for a given triangulation. The action-angle coordinates give a map $\alpha : \mathcal{P} \times T^3 \rightarrow \text{Pol}(6)/\mathbf{SO}(3)$. Cantarella and Shonkwiler prove that the space parametrized by the interior of \mathcal{P} and the 3-torus is a toric symplectic manifold,

call this space $\widehat{\text{Pol}(6)}$. Thus we can apply theorem 10 to show that α restricted to the interior of the moment polytope is a measure preserving map. This means that one can randomly sample points from $\widehat{\text{Pol}(6)}$ by randomly sampling points from the interior of the moment polytope and the 3-torus. This vastly simplifies the process of generating random equilateral hexagons.

In addition, the space $\widehat{\text{Pol}(6)}$ is actually the “correct” space for our purposes. The physical configuration and knot type is invariant under translation and rotation, and $\widehat{\text{Pol}(6)}$ is the space of equilateral hexagons up to translation and rotation.

5 Randomly Generated Knots

Using the action-angle coordinates model given by *Cantarella* and *Shonkwiler* (2016), we randomly generated approximately 50 million knots, and proceeded to categorize them into knot type. This gave valuable insight into the actual location of knots within the moment polytope and the rarity of them. We found only 6,915 trefoils, which estimates that approximately 0.01383% of all hexagonal knots are trefoils.

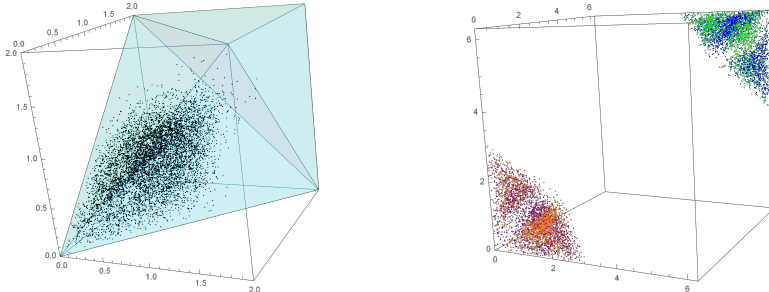


Figure 10: Action-Angle coordinates corresponding to 6915 randomly generated trefoils (colored by trefoil type in T^3).

The action-angle coordinates make sampling random equilateral hexagons surprisingly easy. We uniformly selected d_1, d_2 , and d_3 from the range $[0, 2]$ and θ_1, θ_2 , and θ_3 from the range $[0, 2\pi]$. We then threw out any points that lay outside \mathcal{P} , which is approximately half since \mathcal{P} has volume 4. So although we generated 100 million values, only about 50 million corresponded to knots. We then convert from action-angle coordinates to the 6 vertices in \mathbb{R}^3 .

To test if each given equilateral hexagon was a trefoil we needed to confirm that the three triangular discs (T_2, T_4 , and T_6) were each pierced by another edge of the knot. The exact edges that pierced and the value of the θ 's would allow us to deduce the exact type of trefoil. To accomplish all of this we would need a formula to tell us whether a given edge pierced a triangular disc, which we could then run on each potential edge and triangular disc pairing.

We will describe this with the example of checking if edge $\overline{45}$ pierces T_2 , but the method generalizes easily to all other edge and triangular disc pairings. We first want to find the intersection of $\overline{45}$ with the plane that contains T_2 . We do this with a parametric definition of the plane and the line $\overline{45}$ in terms of variables u , w , and t respectively. We define the plane by $v_1 + (v_2 - v_1) \cdot u + (v_3 - v_1) \cdot w$. We define the line by $v_4 + (v_5 - v_4) \cdot t$. Next we set them equal to each other and solve for values u^* , w^* and t^* . This value for t allows us to compute the exact coordinates of a point p , which is where $\overline{45}$ intersects the plane. We get $p = v_4 + (v_5 - v_4) \cdot t^*$.

Finally we need to determine if p is within the triangle T_2 or if it is elsewhere in the plane. We consider three matrices: $[\vec{p}, \vec{v}_1, \vec{v}_2]$, $[\vec{p}, \vec{v}_2, \vec{v}_3]$, and $[\vec{p}, \vec{v}_3, \vec{v}_1]$. If the determinant of each of these matrices has the same sign, then p is inside of T_2 , thus indicating that $\overline{45}$ pierces T_2 .

6 Results

To bound the knotting probability of equilateral hexagons we consider the moment polytope and the 3-torus separately. The following lemma will be helpful in allowing us to draw conclusions about knots based on their projections. It tells us that if we have a projection in which two triangles don't intersect each other, neither triangle pierces the other in \mathbb{R}^3 .

Lemma 12. *Let A and B be two triangles in \mathbb{R}^3 . Let P be a projection onto some plane. Then if $P(\text{int}(A)) \cap P(\text{int}(B)) = \emptyset$, $\text{int}(A) \cap \text{int}(B) = \emptyset$.*

Proof. Assume otherwise. Then there is at least one point $p \in \text{int}(A) \cap \text{int}(B)$. Let $P(p) = h$. Since p is in $\text{int}(A)$ and $\text{int}(B)$, h must be in $P(\text{int}(A))$ and $P(\text{int}(B))$, so $P(\text{int}(A)) \cap P(\text{int}(B)) \neq \emptyset$, contradicting our initial assumption. \square

6.1 Bounding the angles $(\theta_1, \theta_2, \theta_3)$

We can significantly narrow down the knotting probability by considering which values of θ_1 , θ_2 , and θ_3 always correspond to unknots, regardless of the values d_1 , d_2 , and d_3 .

Theorem 13. *Let $H \in \mathfrak{Eqr}^{(6)} / (\mathbf{SO}(3) \times \mathbb{R}^3)$ be parameterized with our action-angle coordinates $(d_1, d_2, d_3, \theta_1, \theta_2, \theta_3)$. If at least two θ values are between $\frac{\pi}{2}$ and $\frac{3\pi}{2}$ then the hexagon will be an unknot.*

Proof. Let H be an equilateral hexagon in standard position. That is \mathcal{T} , the triangle spanned by v_1 , v_3 , and v_5 , is oriented counter-clockwise in the xy -plane. In order to have a trefoil, it must be true that (among other things) either *Case 1*: T_4 is pierced by $\overline{12}$ and T_6 is pierced by $\overline{34}$, or that *Case 2*: T_4 is pierced by $\overline{61}$ and T_6 is pierced by $\overline{23}$. Hence, in order to have a trefoil we must have the



Figure 11: A hexagon with two θ 's at $\pi/2$.

triangles T_4 and T_6 interlaced, to satisfy the requirement that either $\overline{61}$ pierces T_4 or $\overline{34}$ pierces T_6 .

Vary θ_2 from $\frac{\pi}{2}$ to π . As T_4 rotates from perpendicular to planar (on the exterior) with respect to \mathcal{T} , consider the line drawn by continually projecting v_4 onto the xy -plane, shown as a dotted line in figure 12. Starting at $\theta_2 = \frac{\pi}{2}$, v_4 will project directly onto the edge of \mathcal{T} from v_3 to v_5 . As we rotate T_4 , this projection will only move outward from \mathcal{T} .

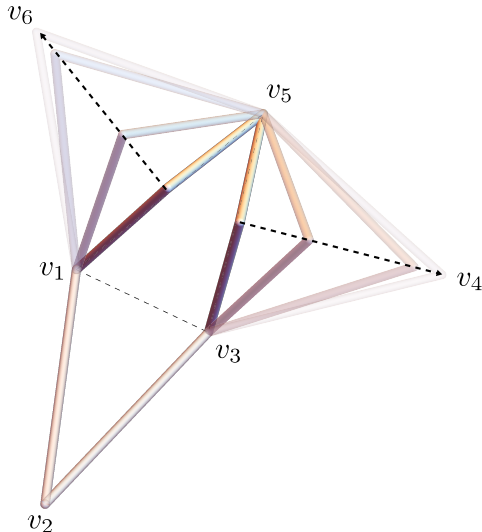


Figure 12: The projections of v_4 and v_6 as θ_2 and θ_3 vary from $\pi/2$ to π .

The same process can be done for θ_3 and T_6 . As seen in Figure 12, these two lines extend outward, each perpendicular to a different side of \mathcal{T} . So they must have between 0 and π degrees between each other, telling us that they will not intersect.

Hence, by Theorem 12, since the projections of v_4 and v_6 over the range $[\frac{\pi}{2}, \pi]$ don't intersect, the triangles can't possibly have edges that pierce each other, and so the configuration is unknotted.

This entire result holds for when at least two θ 's are between π and $\frac{3\pi}{2}$ as well, as that situation is geometrically identical, just reflected down across the

xy -plane. Thus we can conclude that if any two θ 's are within $[\frac{\pi}{2}, \frac{3\pi}{2}]$ then we have an unknot. \square

Theorem 14. *The portion of the 3-torus in which hexagonal equilateral trefoils can occur has a volume of at most $\frac{1}{8}$ of the total volume.*

Proof. Think of points on the 3-torus as coordinates within the $2\pi \times 2\pi \times 2\pi$ cube. The coordinate value in each dimension tells us how far around that axis of the 3-torus we are, and each corresponds to one of θ_1 , θ_2 , or θ_3 . We can split this cube up into 8 cubes each of sidelength π . In order to have a trefoil, we must have all three vertices v_2 , v_4 , and v_6 together above \mathcal{T} or together below (recall curl). Hence we can rule out 6 of the 8 cubes, leaving only $[0, \frac{\pi}{2}] \times [0, \frac{\pi}{2}] \times [0, \frac{\pi}{2}]$, and $[\pi, \frac{3\pi}{2}] \times [\pi, \frac{3\pi}{2}] \times [\pi, \frac{3\pi}{2}]$. Let's consider only the first (and all our findings will hold for the other due to symmetry).

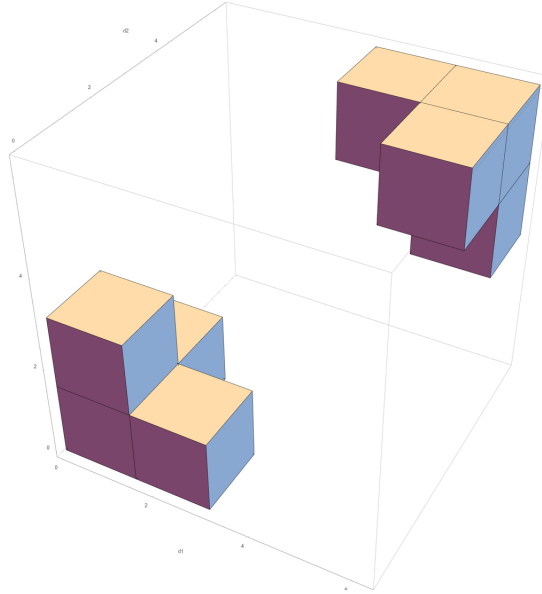


Figure 13: The region \mathcal{S} of the 3-torus where knots can occur.

See Figure 13. We can split this up into 8 smaller cubes each of side length $\frac{\pi}{2}$. Only 4 of these 8 cubes contain points satisfying the constraint imposed by Theorem 14. The four of them are $[0, \frac{\pi}{2}] \times [0, \frac{\pi}{2}] \times [\frac{\pi}{2}, \pi]$ and $[0, \frac{\pi}{2}] \times [\frac{\pi}{2}, \pi] \times [0, \frac{\pi}{2}]$ and $[\frac{\pi}{2}, \pi] \times [0, \frac{\pi}{2}] \times [0, \frac{\pi}{2}]$ and $[0, \frac{\pi}{2}] \times [0, \frac{\pi}{2}] \times [\frac{\pi}{2}, \pi]$. Symmetrically, we have four cubes in the opposite corner corresponding to the case where curl is negative. Thus we have narrowed down to $\frac{1}{4}$ of the original space, and from there cut it in half again, so trefoils can be created within at most $\frac{1}{8}$ of the original volume. \square

6.2 Bounding diagonal lengths (d_1, d_2, d_3)

Consider an equilateral hexagon with all side lengths equal to 1 such that when each of the three triangles T_2 , T_4 , and T_6 are rotated all the way in to $\theta = 0$ or $\theta = \pi$, adjacent edges completely overlap. Then the triangle \mathcal{T} described by the action coordinates has circumcenter where v_2 , v_4 , and v_6 coincide and can be inscribed in a circle of radius 1.

Lemma 15. *Let $H \in \mathfrak{Eqr}^{(6)}/(\mathbf{SO}(3) \times \mathbb{R}^3)$ be parameterized with our action-angle coordinates $(d_1, d_2, d_3, \theta_1, \theta_2, \theta_3)$. Consider a triangle inscribed in a circle of radius 1, with side lengths a , b , and c , where c is the length of the longest side. Then, if $a = d_1$, $b = d_2$, and $d_3 > c$, then the hexagon must be an unknot.*

Proof. Let O denote the circumcenter at ($O = v_2 = v_4 = v_6$) and let $\angle xyz$ denotes the angle $v_x v_y v_z$. Recall that \mathcal{T} denotes the triangle spanned by v_1, v_3 , and v_5 .

Case 1: Shown in Figure 14. The circumcenter is inside triangle \mathcal{T} . In this case, increasing d_3 while holding the other side lengths constant causes $\angle 135$ to increase. Since the side lengths of T_2 and T_4 are fixed, $\angle 53O$ and $\angle O31$ are fixed as well. Therefore, increasing d_3 causes the angles to separate so that triangles T_2 and T_4 coincide only at the point v_3 .

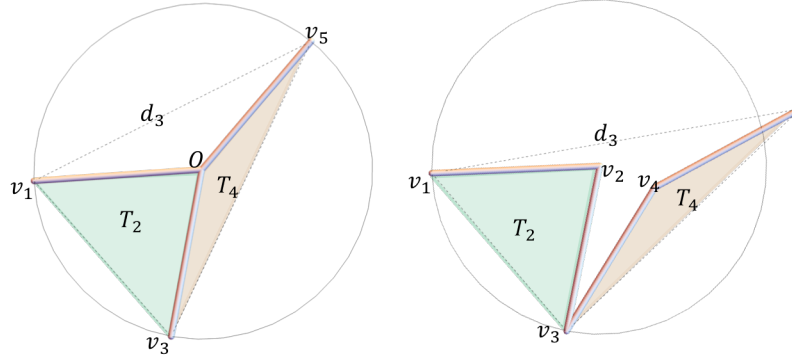


Figure 14: Case 1 in the proof of Lemma 8, when the circumcenter is inside the triangle. The image on the left shows when $d_3 = c$ and the image on the right shows when $d_3 > c$ so T_2 and T_4 are separated.

Case 2: Shown in Figure 15. The circumcenter is outside the triangle \mathcal{T} . Since d_3 is the longest side, v_1 must be located on the smaller arc bounded by d_3 . Otherwise, d_1 or d_2 will be longer than d_3 . Thus, the edge where $\overline{12}$ and $\overline{61}$ coincide must intersect d_3 . Increasing the length of d_3 while holding the

other lengths constant will cause $\angle 513$ to increase while $\angle 516$ and $\angle 213$ remain constant. Then the triangles coincide only at v_1 .

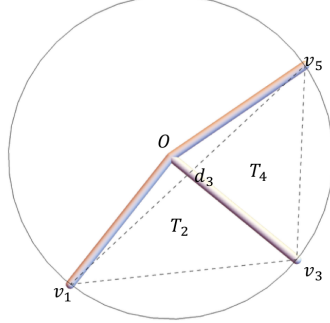


Figure 15: Case 2 in the proof of Lemma 8, when the circumcenter is outside of the triangle.

In either case, if $d_3 > c$ then two of the triangles in the projection are disjoint. In order for a hexagon to be knotted, for each pair of triangles in T_2, T_4, T_6 , one must pierce the other or vice versa. By Theorem 12 if two triangles don't intersect in the projection of a knot, neither can be pierced by the other and the hexagon must be unknotted.

Furthermore, if in \mathcal{T} the triangles T_2 and T_4 don't overlap when they are folded in to $\theta = 0$, then they can't overlap for any angles. To see this, consider the projection of T_2 and T_4 . Figure 16 shows the process of folding out T_2 and T_4 to any angle. The vertex v_2 moves along the perpendicular bisector of $\overline{13}$, and similarly the vertex v_4 moves along the perpendicular bisector of $\overline{35}$. Thus for no angles can the interiors of two triangles overlap.

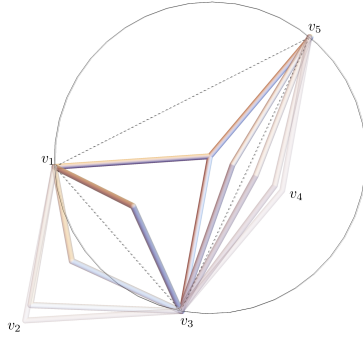


Figure 16: Angles folding out from $\theta = 0$, showing that the distance between T_2 and T_4 increases.

□

Theorem 16. *The portion of the moment polytope in which hexagonal equilateral trefoils can occur has a volume of at most π .*

Proof. For any triangle inscribed in a circle of radius 1, the following relationship derived from the law of cosines holds between the side lengths a , b , and c :

$$c^2 = a^2 + b^2 - 2ab \arccos \frac{c}{2} = a^2 + b^2 - 2ab\sqrt{4 - c^2} \quad (4)$$

This equation is symmetric with respect to a , b and c , so they can correspond to any permutation of d_1 , d_2 and d_3 . Given two side lengths a and b , solving the previous equation gives us an upper value for c , which we call U_c , and a lower value of c , which we call L_c . These equations describe all tuples (a, b, c) corresponding to an inscribed triangle.

$$U_c = \frac{a}{2}\sqrt{4 - b^2} + \frac{b}{2}\sqrt{4 - a^2} \quad (5)$$

$$L_c = \left| \frac{a}{2}\sqrt{4 - b^2} - \frac{b}{2}\sqrt{4 - a^2} \right| \quad (6)$$

$U_c > L_c$ and $L_c < a$ for all values of a , b and c , meaning the surface produced by the L_c equation will not be in the region where c is the longest side, so we don't need to consider it. Some portion of the surface produced by the U_c equation will be in the region where c is the longest length, and this is the portion we will consider.

We can divide the moment polytope into 6 sections depending on the relative lengths of the sides: one such is the region where $c > b > a$, and the others are all the permutation of the variables in that inequality. Given the symmetric nature of the polygons, we will only consider the region where $c > b > a$. Any conclusions drawn about this region can be extended to the other 5 regions where the lengths are ordered differently. Figure 17 shows the one of the 6 regions where $d_3 > d_2 > d_1$ and $d_3 < U_c$.

Putting the 6 symmetric sections together, we get a region contained in the moment polytope shown in figure 18. We call this region \mathcal{R} . Given a and b , U_c tells us the maximum value for c before we are guaranteed an unknot. So we seek to find the volume where $c < U_c$ and $c > b > a$ within the moment polytope. To do this we compute the following integral:

$$\int_{a=0}^{\sqrt{3}} \int_{b=a}^{\sqrt{2+\sqrt{4-a^2}}} \frac{a}{2}\sqrt{4-b^2} + \frac{b}{2}\sqrt{4-a^2} - b \, dbda = \frac{\pi}{6} \quad (7)$$

This is the volume of the region shown in figure 17. Now let us consider the disjoint region where $c > a > b$. We can do a nearly identical integral, just with a and b swapped, and will find that region's volume to be $\frac{\pi}{6}$ as well. Finally, we can derive U_a and U_b in the same way as we derived U_c . This gives analogous integrals for the remaining 4 regions.

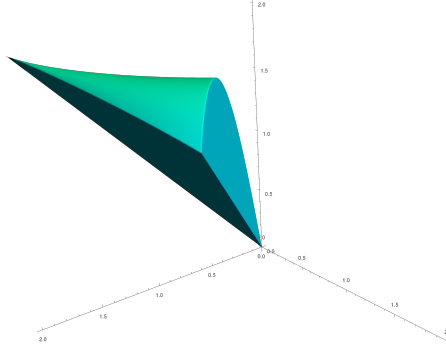


Figure 17: Section of the moment polytope where $d_3 > d_2 > d_1$ and $d_3 < U_c$.

Altogether the moment polytope was divided into 6 regions, and bounding each of them resulting in volumes of $\frac{\pi}{6}$. Thus the total volume of the region where (d_1, d_2, d_3) can correspond to trefoils is bounded above by π . \square

6.3 Our Bound on the Knotting Probability

We have bounded the region of potential trefoils in the moment polytope to just volume π . The polytope has a volume of 4, so the proportion that can correspond to trefoils is $\pi/4$. We have also bounded the proportion of potential trefoils in the 3-torus to $1/8$. Because the map from these regions to the space of equilateral hexagons is measure preserving, we can bound the proportion of possible trefoils by simply multiplying together these values.

Theorem 17. *The probability that a randomly generated hexagon is a trefoil is at most $\frac{\pi}{32}$.*

Proof. The knotting probability is the expected value of the function

$$\chi(H) = \begin{cases} 1 & \text{if } H \text{ is a trefoil} \\ 0 & \text{if } H \text{ is an unknot} \end{cases}$$

over all of the non-singular equilateral hexagons in $\widehat{\mathfrak{E}\mathfrak{qu}(6)} = \mathfrak{E}\mathfrak{qu}(6)/(\mathbf{SO}(3) \times \mathbb{R}^3)$. ($\widehat{\mathfrak{E}\mathfrak{qu}(6)}$ is parametrized using the T_{135} triangulation and the action angle map defined in Section 4.) More precisely, this expected value is

$$\mathbb{E}(\chi) = \frac{\int_{\widehat{\mathfrak{E}\mathfrak{qu}(6)}} \chi}{\int_{\widehat{\mathfrak{E}\mathfrak{qu}(6)}} 1}$$

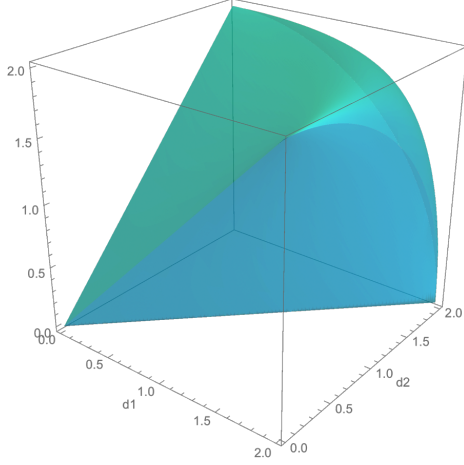


Figure 18: \mathcal{R} , the region of the moment polytope where $d_3 < U_c, d_2 < U_c$, and $d_1 < U_c$.

We know that for any $(d_1, d_2, d_3, \theta_1, \theta_2, \theta_3)$, $\chi(d_1, d_2, d_3, \theta_1, \theta_2, \theta_3)$ is bounded above by

$$g(d_1, d_2, d_3, \theta_1, \theta_2, \theta_3) = \begin{cases} 1 & \text{if } (d_1, d_2, d_3) \in \mathcal{R} \text{ and } (\theta_1, \theta_2, \theta_3) \in \mathcal{S} \\ 0 & \text{otherwise.} \end{cases}$$

Let \mathcal{R} be the region of the polytope which could contain trefoils (defined in the proof of theorem 16), and let \mathcal{S} be the region of the cube which could contain trefoils defined in the proof of theorem 14 . Then we can write g as $g_d \cdot g_\theta$ where

$$g_d(d_1, d_2, d_3) = \begin{cases} 1 & \text{if } (d_1, d_2, d_3) \in \mathcal{R} \\ 0 & \text{otherwise} \end{cases}, \text{ and}$$

$$g_\theta(\theta_1, \theta_2, \theta_3) = \begin{cases} 1 & \text{if } (\theta_1, \theta_2, \theta_3) \in \mathcal{S} \\ 0 & \text{otherwise.} \end{cases}.$$

So we can use Theorem 10 to find that

$$\mathbb{E}(g) = \frac{\int_{\mathcal{P}} g_d(d_1, d_2, d_3) d\text{Vol}_{\mathbb{R}^3} \cdot \int_{T^3} g_\theta(\theta_1, \theta_2, \theta_3) d\theta_1 d\theta_2 d\theta_3}{\int_{\mathcal{P}} 1 d\text{Vol}_{\mathbb{R}^3} \cdot \int_{T^3} 1 d\theta_1 d\theta_2 d\theta_3} = (\pi/4) \cdot (1/8) = \pi/32$$

Thus this knotting probability of a random equilateral hexagon is $\mathbb{E}(\chi) \leq \mathbb{E}(g) = \pi/32$. □

Our bound is approximately 0.098, in contrast to the 0.5 bound that was given in previous literature. We clearly have a vast improvement, but as our simulations show the bound could still be improved drastically.

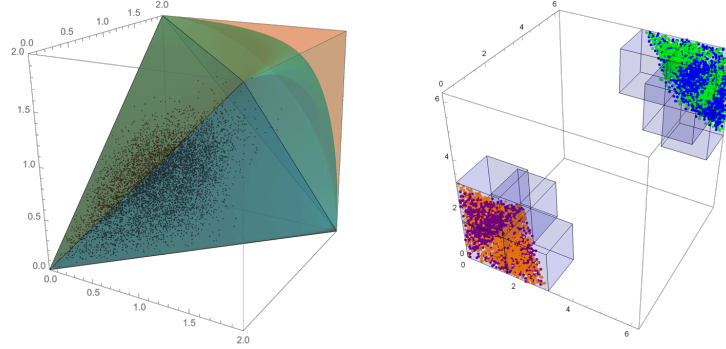


Figure 19: The bounded region \mathcal{R} contained in the moment polytope \mathcal{P} with the points generated by the experiment (left), and the 3-torus \mathcal{T}^3 with the bounded region S and the points sampled by the experiment (right).

7 Bibliography

- C. Adams, *The Knot Book: An elementary introduction to the mathematical theory of knots*, AMS, 2001
- J. Cantarella and C. Shonkwiler, The symplectic geometry of closed equilateral random walks in 3-space, *Ann. Appl. Probab.* 26 (02, 2016) 549–596.
- J. A. Calvo, Geometric knot spaces and polygonal isotopy, *Journal of Knot Theory and Its Ramifications* 10 (2001), no. 02 245–267.